

DYNAMICS OF THE ALPHA PEAK FREQUENCY DURING FLICKER STIMULATION

Gary Garcia-Molina¹, Piotr Milanowski²

¹Philips Research Europe
High Tech Campus 34, 5656AE, Eindhoven, The Netherlands
gary.garcia@philips.com

²Laboratory of Medical Physics
Institute of Experimental Physics
Warsaw University, Hoża 69, 00-681 Warszawa, Poland
piotr.milanowski@gmail.com

ABSTRACT

Repetitive visual stimulation elicits specific brain responses known as steady state visual evoked potentials (SSVEP). The SSVEP manifests as oscillatory components at the stimulation frequency or harmonics in brain signals such as the electroencephalogram (EEG) or magnetoencephalogram. Analysis of the dynamics of the SSVEP permits to characterize the neurophysiological basis of visual processing. Classical SSVEP analysis is restricted to the study of the EEG power at the stimulation frequency. In this paper, we focus on the dynamics of the alpha peak frequency under flicker stimulation. The alpha peak frequency is person specific and plays an important role on mental load. High resolution time-frequency methods are necessary to precisely identify the alpha peak frequency. We utilize therefore matching pursuit methods using stochastic dictionaries. We show that the alpha peak frequency decreases during flicker stimulation. We argue that this phenomenon can partially explain the relative fast habituation of the SSVEP, i.e. the strength of the SSVEP decreases after few seconds of continuous flicker stimulation.

1. INTRODUCTION

Stimulation by repetitive light flashes (flickering) is a widely used method to study the visual processes in the brain. The steady state visual evoked potential (SSVEP) refers to the activity of the cerebral cortex that results from attending to a repetitive visual stimulus (RVS) oscillating at a constant *stimulation frequency*. The SSVEP can be observed in the scalp recorded electroencephalogram (EEG) as oscillatory components at the stimulation frequency and/or harmonics (see Figure 1). The SSVEP is more prominent at parietal and occipital locations due to their relative proximity to the primary visual cortex [1].

In SSVEP research, the EEG components at the stimulation frequency are generally characterized. However the SSVEP is also accompanied by other phenomena in the brain which can be characterized by the dynamics in the alpha frequency (8-12 Hz). Of particular importance is the alpha peak frequency which corresponds to the frequency in the alpha band where the EEG power is maximum [2].

This paper focuses on the dynamics of the alpha peak frequency during flicker stimulation. As it was already shown in [3, 4], the alpha peak frequency increases with increasing mental load. Other studies have shown that the alpha peak frequency is positively correlated with

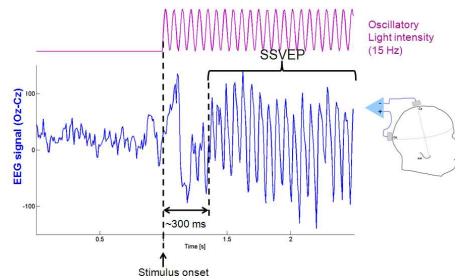


Figure 1: Steady state visual evoked potential (SSVEP) elicited by flicker stimulation at 15 Hz.

intelligence [5] and can be viewed as an indicator of cognitive performance [2].

The analysis of the alpha peak frequency requires a high resolution time-frequency analysis method for the EEG signals. As suggested in [2] the alpha peak frequency is subject dependent and needs customized identification using analysis techniques beyond simple filtering. A high time resolution is also required because of the time synchronization with the flicker stimulation. This paper utilizes the matching pursuit approach using stochastic dictionaries. Section 2 summarizes the basics of the matching pursuit algorithm, Section 3 describes the experimental protocol. In Section 4 we discuss the results and make sense of them under a neurophysiology perspective. The paper conclusions are finally presented in Section 5.

2. SIGNAL PROCESSING METHODS

In this section we briefly present the basics of the matching-pursuit method which is used to analyze the EEG under flicker stimulation. Matching pursuit is an iterative algorithm, originally presented in [6], that approximates a signal $s(t)$ with a set of *atoms*. In each iteration a function from a dictionary of atoms $D = g_1, \dots, g_n$ is chosen so that it satisfies the equation:

$$g_{\gamma_i} = \operatorname{argmax}_{g_{\gamma_i} \in D} \|\langle R_s^i, g_{\gamma_i} \rangle\| \quad (1)$$

where $\langle \cdot, \cdot \rangle$ denotes the inner product operator, i is the iteration index, and R_s^i is a residual left after subtracting the results of previous iterations:

$$\begin{aligned} R_s^0 &= s \\ R_s^n &= \langle R_s^n, g_{\gamma_n} \rangle g_{\gamma_n} + R_s^{n+1} \end{aligned} \quad (2)$$

The dictionary D is constructed from Gabor (sine-modulated Gaussian functions) atoms because they provide optimal joint time-frequency localization.

$$g_\gamma(t) = K(\gamma) \exp^{-\pi \frac{(t-u)^2}{\sigma^2}} \cos(2\pi f(t-u) + \phi) \quad (3)$$

where the argument γ denotes the set of parameters $\{u, f, \sigma, \phi\}$ which are the time shift (translation), frequency, scale, and phase respectively. The term $K(\gamma)$ is a normalization parameter so that $\|g_\gamma\| = 1$.

If the dictionary D is complete, it is possible to prove [6] that:

$$\begin{aligned} s(t) &= \sum_{i=1}^{\infty} \langle R_s^i, g_{\gamma_i} \rangle g_{\gamma_i} \\ \|s(t)\|^2 &= \sum_{i=1}^{\infty} |\langle R_s^i, g_{\gamma_i} \rangle|^2 \end{aligned} \quad (4)$$

In practice, finite dictionaries having M elements, are used. A signal $s(t)$ is then approximated by the decomposition:

$$s(t) \approx \sum_{i=1}^M \langle R_s^i, g_{\gamma_i} \rangle g_{\gamma_i} \quad (5)$$

The coefficients $\langle R_s^i, g_{\gamma_i} \rangle$ can be considered as amplitudes of atoms g_{γ_i} in the signal $s(t)$.

2.1 Stochastic dictionaries

Constructing the dictionary D requires sampling in the parameter space $\{t, f, \sigma\}$. The phase ϕ can be optimized in each step of the decomposition procedure separately for each fitted atom [7]. Using any fixed scheme of sampling in the parameter space introduces statistical bias in the resulting parametrization. To address this, the use of stochastic dictionaries was proposed in [7]. To define a dictionary D , a space of parameters $\{t, f, \sigma\}$ is divided into "cubes" of size $\Delta\sigma$, Δt and Δf , where the resolution $(\Delta\sigma, \Delta t, \Delta f)$ is set before the procedure. In each of these cubes a single atom is chosen by drawing its parameters from flat distributions within the given ranges of continuous parameters.

The first iteration reduces the dictionary Δ to a subset Δ_α constructed by selecting an arbitrary percentage of atoms having largest correlations with the original signal. The atom g_{γ_i} chosen in each iteration from the dictionary Δ_α (or Δ in the first iteration), is optimized further by a search in a dense dictionary D_{γ_i} constructed from parameters in the neighborhood of γ_i .

2.2 Energy distribution

The decomposition based on the matching pursuit approach, provides a simple method to remove the typical cross-terms in the Wigner-Ville distribution [7, 8]. Using the atomic decomposition in (4) of $s(t)$, the Wigner-Ville distribution (WVD) of $s(t)$ can be written as:

$$\begin{aligned} W_s(t, f) &= \sum_{i=1}^{\infty} |\langle R_s^i, g_{\gamma_i} \rangle|^2 W_{g_{\gamma_i}}(t, f) + \\ &+ \sum_{i=1}^{\infty} \sum_{j=0, j \neq i}^{\infty} \langle R_s^i, g_{\gamma_i} \rangle \langle R_s^j, g_{\gamma_j} \rangle W[g_{\gamma_i}, g_{\gamma_j}](t, f) \end{aligned} \quad (6)$$

where W denotes the WVD. The second term on the right in (6) corresponds to WVD cross-terms. Removing

them is simply a matter of defining the time-frequency energy distribution of $s(t)$ as:

$$E_s(t, f) = \sum_{i=1}^{\infty} |\langle R_s^i, g_{\gamma_i} \rangle|^2 W_{g_{\gamma_i}}(t, f) \quad (7)$$

This is possible since the WVD satisfies

$$\int_{-\infty}^{\infty} \int_{-\infty}^{\infty} W_g(t, f) dt df = \|g\| = 1, \quad (8)$$

and (4) implies conservation of energy:

$$\int_{-\infty}^{\infty} \int_{-\infty}^{\infty} E_s(t, f) dt df = \|s\| \quad (9)$$

$E_s(t, f)$ can therefore be interpreted as an energy density of s in the time-frequency plane. This is also illustrated in Figure 3.

3. EXPERIMENTAL PROTOCOL

Three male subjects (S1, S2, and S3), aged ages 24, 29, and 31, participated in this experiment. They were requested to seat in front of a lamp positioned approximately one-meter away from their eyes. The lamp consisted of twelve LEDs, arranged in a 3x4 configuration, which shone through a white diffusion screen. The color temperature was of 4441.3K and the light luminance in the "on" state was of 460 Cd/m².

Subjects were presented with repetitive visual stimulation at 14 frequencies: 19Hz, 20Hz, 24Hz, 25Hz, 27Hz, 29Hz, 30Hz, 32Hz, 34Hz, 35Hz, 37Hz, 39Hz, 40Hz, and 45Hz. These were presented in four sessions. In the first three sessions, four stimulation frequencies (randomly selected) were used and in the fourth session two stimulation frequencies. Each stimulation frequency was presented once only. The sessions took place at around the same time of the day (early afternoon) to avoid circadian influences on the measurements.

The presentation of a given stimulation frequently was divided into thirty intervals which comprised a 4-second long stimulation period where the lamp flickered followed by a break period of random duration between 15 and 20 seconds (see Figure 2a). Such relatively long break period was chosen in order to ensure that consecutive stimulation periods are independent from each other. Indeed, as discussed in [9], the amplitude of the SSVEP decreases if the stimulation periods are too close from each other. Two seconds before the onset of each flickering stimulus, a warning sound was played so that the subject could avoid artifacts due to head or ocular movements. This signal also reduced expectancy effects on the alpha band [2].

The EEG data of subjects was collected using an Active2 Biosemi system [10] at the 32 locations that are shown in Figure 2b at a sampling rate of 2048 Hz. The analysis was performed on electrode Oz because the SSVEP manifests more prominently at this site [11]. To obtain a reference free signal at Oz, common average re-referencing [12] was applied, i.e. subtracting from the

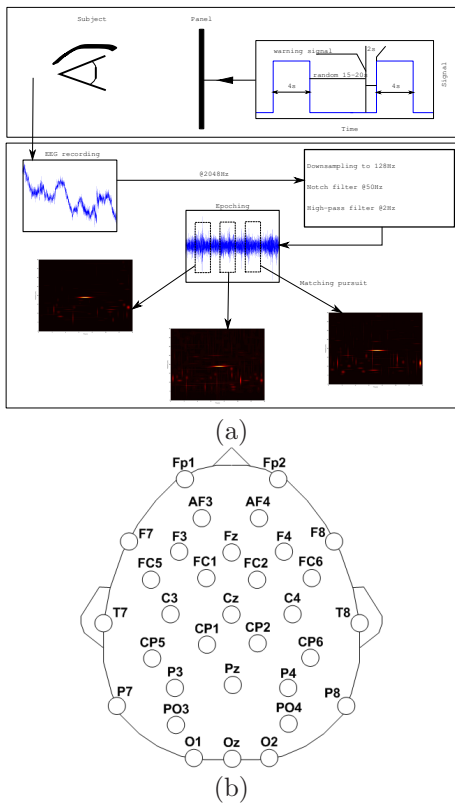


Figure 2: (a) Experimental protocol. (b) EEG recording sites.

Oz signal, the average of the signals at all 32 sites. The resulting signal was then band-pass filtered in the 2-50 Hz band and sub-sampled at 128 Hz. The analysis was conducted in epochs starting 5 seconds before stimulation onset and ending 5 seconds after the stimulation ended.

4. RESULTS AND DISCUSSION

To illustrate the effect of the time-frequency representation (TFR) method on the analysis of EEG during flicker stimulation, we report in Figure 3 the time-frequency analysis of the EEG epochs during flicker stimulation at 19 Hz for subject S2. The TFR images result from averaging over the 30 recorded epochs.

The vertical lines in Figure 3 at 5 and 9 seconds mark the beginning and the end of the stimulation respectively. We present the TFRs associated with the short-time Fourier transform using a 4-second long window [13] (Figure 3a), the smoothed Wigner-Ville transform [13] (Figure 3b), a 30-order autoregressive modeling in a 4-second long window [14] (Figure 3c), and the matching pursuit TFR (MP-TFR) (Figure 3d). The latter provides the most meaningful time-frequency representation from a neurophysiological standpoint. Indeed, the SSVEP start few hundreds of milliseconds (see also Figure 1) after stimulation onset and habituates (diminishes in amplitude) after around three seconds [1].

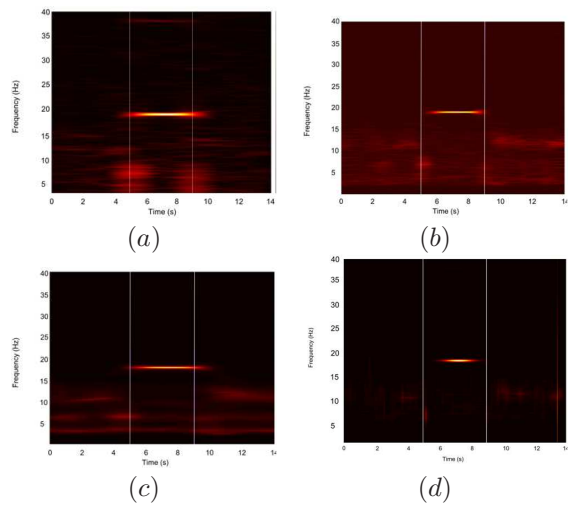


Figure 3: Average TFRs of the EEG epochs of subject S2 for flicker stimulation at 19 Hz. The vertical lines signal the beginning and end of the stimulation. (a) Short-time Fourier transform. (b) Smoothed Wigner-Ville transform. (c) Autoregressive modeling. (d) Matching pursuit.

4.1 Alpha peak frequency

To determine the alpha-peak frequency from the MP-TFR in a given interval, the following procedure was followed. We first selected the atoms localized within the targeted time interval, lasting for at least 100 milliseconds, and having a central frequency in the 8 to 12 Hz range. The alpha-peak frequency results then from a weighted average of the selected atoms frequencies weighted by their respective amplitude (see (5)).

For each subject, we first estimated the alpha peak frequency in the absence of flicker stimulation. This step consisted in selecting for each epoch, the atoms localized in the time interval spanning from 1 to 3 seconds. The alpha peak frequency resulted then from computing the grand average across all epochs and trials. The resulting individual alpha peak frequencies (IAF) are reported in Table 1.

Subject	S1	S2	S3
IAF (Hz)	11.02 ± 0.08	10.42 ± 0.05	10.21 ± 0.09

Table 1: Individual alpha peak frequencies in the absence of flicker stimulation.

4.2 Alpha peak frequency during the stimulation

The alpha peak frequency during the stimulation period (seconds from 5 to 9) were estimated similarly to the procedure described in Section 4.1.

The SSVEP time course for each flicker stimulation frequency was determined by: i) applying a narrow band filter centered around the stimulation frequency on the signal recorded at Oz, ii) squaring the resulting signal, and iii) applying a soothing running average filter.

The time courses of the alpha peak frequency during flicker stimulation for subject S2 and all stimulation

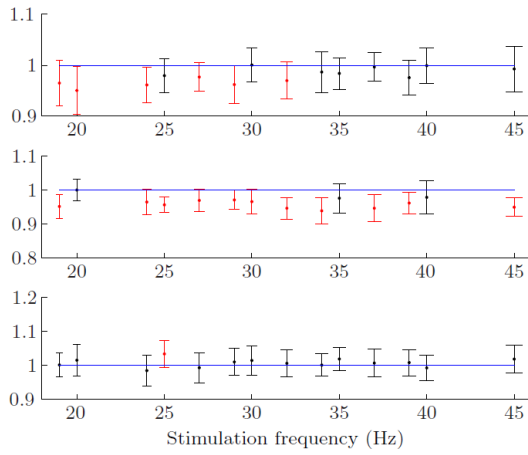


Figure 5: Average ratios (and corresponding error bars) between the alpha peak frequency during flicker stimulation and the IAF. The red colored bars indicate the ratios that statistically significantly differ from the unity. Top: subject S1, Middle: subject S2, and bottom: subject S3.

frequencies are depicted in Figure 4. With the exception of the curves for the flicker stimulation at 20 Hz, the alpha peak frequency decreases after stimulation onset, reaches a minimum, and starts increasing around 3 seconds after stimulation onset, i.e. when the SSVEP response starts to habituate, i.e. the amplitude of the SSVEP decreases.

To test this trend, we have computed the average ratio between the alpha peak frequency during stimulation and the IAF (see Section 4.1). For each stimulation frequency, a Wilcoxon test [15] was used to test whether resulting ratios were significantly different from unity. Figure 5 shows the average ratios (and the corresponding error bars) for all stimulation frequencies and subjects. The bars in red indicate statistically significant values. Due to the multiple comparison problem, the single case significance level was decreased using Bonferroni corrections [16] from 0.01 to $\frac{0.01}{14} = 7.14 \cdot 10^{-4}$. Subjects S1 and S2 exhibit a significant decrease of the alpha peak frequency during flicker stimulation.

To assess if the SSVEP dynamics and that of the alpha peak frequency evolve in opposite directions during flicker stimulation, we have computed the Kendall correlation coefficient [17] between the time courses of the SSVEP and the alpha peak frequency for each subject and stimulation frequency. The results are reported in Table 2. As it can be seen, the opposite evolution trend, i.e. the SSVEP increases while the alpha peak frequency decreases and vice-versa, does hold for subject S5 and to a lesser extent for subject S6.

5. CONCLUSIONS

In [3, 4] it is suggested that the alpha peak frequency is positively correlated with mental task difficulty. In this paper, most of the statistically significant results (see Figure 5) indicate that the alpha peak frequency decreases during flicker stimulation. Following the logic in [3, 4], this seems to indicate a low brain process-

Freq. (Hz)	S1	S2	S3
19	-0.45 (0.00)	0.19 (0.00)	-0.44 (0.00)
20	0.70 (0.00)	-0.09 (0.00)	-0.01 (0.76)
24	0.30 (0.00)	-0.21 (0.00)	-0.25 (0.00)
25	0.22 (0.00)	-0.07 (0.00)	-0.03 (0.17)
27	0.28 (0.00)	-0.62 (0.00)	-0.21 (0.00)
29	0.30 (0.00)	-0.60 (0.00)	0.17 (0.00)
30	0.43 (0.00)	-0.36 (0.00)	0.19 (0.00)
32	0.12 (0.00)	-0.60 (0.00)	-0.25 (0.00)
34	0.21 (0.00)	-0.69 (0.00)	-0.39 (0.00)
35	0.33 (0.00)	-0.11 (0.00)	-0.28 (0.00)
37	0.37 (0.00)	0.12 (0.00)	-0.14 (0.00)
39	-0.19 (0.00)	-0.37 (0.00)	0.56 (0.00)
40	0.01 (0.60)	-0.44 (0.00)	-0.41 (0.00)
45	-0.16 (0.00)	-0.11 (0.00)	-0.32 (0.00)

Table 2: Kendall correlation between SSVEP power time course and alpha peak frequency time course. (p-values in parentheses.)

ing load of flickering stimulation. This may provide interesting explanatory elements about the fast habituation of the brain to repetitive stimuli. It is well known that repetitive sensory stimuli are ignored after some time. This paper argues that further studies of this phenomenon using the alpha peak dynamics are needed.

The analysis presented in this paper was made possible by the utilization of high resolution matching pursuit methods. As shown in Figure 3, the MP-TFR provides the representation that most closely reflects the neurophysiologic processes in the brain under flicker stimulation.

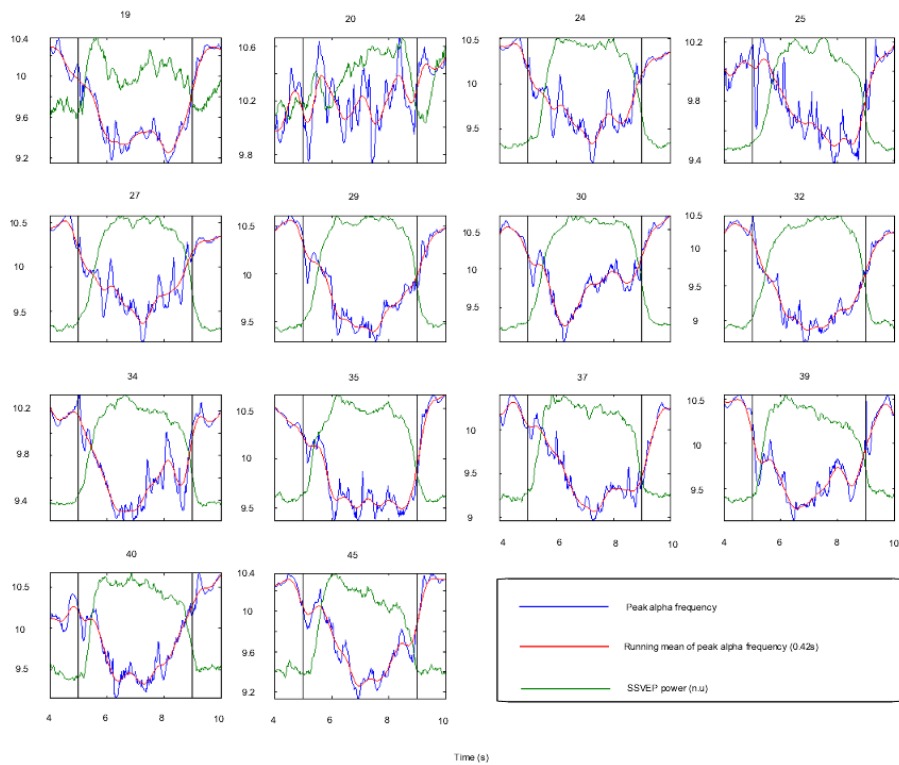


Figure 4: Time courses of the alpha peak frequency for subject S2 at all flicker stimulation frequencies. In green, the SSVEP power is represented. In blue and red, are respectively represented the time course of the alpha-peak frequency and its smoothed version.

REFERENCES

- [1] D. Regan. *Human Brain Electrophysiology: Evoked Potentials and Evoked Magnetic Fields in Science and Medicine*. Elsevier, 1989.
- [2] W. Klimesch. EEG alpha and theta oscillations reflect cognitive and memory performance: a review and analysis. *Brain research. Brain research reviews*, 29(2-3):169–195, 1999.
- [3] M. Osaka. Peak alpha frequency of EEG during a mental task: task difficulty and hemispheric differences. *Psychophysiology*, 21:101–105, 1984.
- [4] M. Osaka, N. Osaka, S. Koyama, T. Okusa, and R. Kakigi. Individual differences in working memory and peak alpha frequency shift on magnetoencephalogram. *Cognitive Brain Research*, 8:365–368, 1999.
- [5] A. Anokhin and F. Vogel. Eeg alpha rhythm frequency and intelligence in normal adults. *Intelligence*, 23:1–14, 1996.
- [6] S.G. Mallat and Z. Zhang. Matching pursuit with time-frequency dictionaries. *IEEE Transactions on Signal Processing*, 41(12):3397–3415, 1993.
- [7] P.J. Durka, D. Ircha, and K.J. Blinowska. Stochastic time-frequency dictionaries for matching pursuit. *IEEE Transactions on Signal Processing*, 49(3):507–510, 2001.
- [8] P.J. Durka. *Time-frequency analyses of EEG*. PhD thesis, Institute of Experimental Physics Department of Physics Warsaw University, August 1996.
- [9] G. Garcia-Molina and V. Mihajlovic. Spatial filters to detect Steady State Visual Evoked Potentials elicited by high frequency stimulation: BCI application. *Journal of Biomedizinische Technik / Biomedical Engineering*, 55(3):173–182, 2010.
- [10] Biosemi. Biosemi system. <http://www.biosemi.com>.
- [11] M.A. Pastor, J. Artieda, J. Arbizu, M. Valencia, and J.C. Masdeu. Human cerebral activation during steady-state visual-evoked responses. *The Journal of Neuroscience*, 23(37):11621–11627, 2003.
- [12] P.L. Nunez and R. Srinivasan. *Electric Fields of the Brain: The Neurophysics of EEG*. Oxford University Press, 2005.
- [13] L. Cohen. *Time-Frequency Analysis*. Prentice Hall, 1995.
- [14] G. Box, G.M. Jenkins, and G.C. Reinsel. *Time Series Analysis: Forecasting and Control*. Prentice-Hall, 1993.
- [15] F. Wilcoxon. Individual comparisons by ranking methods. *Biometrics Bulletin*, 1(6):80–83, 1945.
- [16] H. Abdi. Bonferroni and Sidak corrections for multiple comparisons. In Neil Salkind, editor, *Encyclopedia of Measurement and Statistics*, pages 103–107. Thousand Oaks (CA), 2007.
- [17] M. Kendall. A New Measure of Rank Correlation. *Biometrika*, 30(1-2):81–89, 1938.